

## **Evaluation on Distributed Renewable Energy System Integrated with a Passive House Building Using a New Energy Performance Index**

**Yang Wang<sup>a,b,1</sup>**, Jens Kuckelkorn<sup>c</sup>, Daoliang Li<sup>a</sup>, Jiangtao Du<sup>d</sup>

- a) College of Information and Electrical Engineering, China Agricultural University,  
Beijing, China
- b) School of the Built Environment and Architecture, London South Bank University,  
London, UK
- c) Division of Technology for Energy Systems and Renewable Energy, Bavarian  
Centre for Applied Energy Research (ZAE Bayern), Munich, Germany
- d) School of the Built Environment, Liverpool John Moores University, Liverpool, UK

---

<sup>1</sup> Author to whom correspondence should be addressed.

**Address:** College of Information and Electrical Engineering, China Agricultural University, Beijing, China

**Contact:** wanghongyang1767@gmail.com, wangy47@lsbu.ac.uk (**Yang Wang**).

## Abstract and keywords

### **Abstract**

The newly built Passive House school buildings have broadly employed a novel distributed renewable energy system for heating energy supply in Germany. This article proposed a distributed renewable energy system and investigated its performances (energy and thermal comfort) through numerical simulations in a school building. A new energy performance index has therefore been defined to evaluate this renewable energy system in the school. The energy system simulation (ESS) methodology and numerical models were validated by typical on-site measurements, including borehole outlet temperature and COP of heat pump. In addition, more numerical simulations relevant to energy performance of the proposed renewable energy system have been conducted based on the effects of the borehole outlet temperature and heat recovery efficiency. Several important findings can be achieved as follows. 1) Increasing the heat recovery efficiency of water-water heat exchanger facility would not only significantly improve COP, but also reduce obviously electricity use and energy costs. 2) A comparison, between the systems with heat recovery efficiency of 0.9 and without heat recovery, demonstrated the reduction of CO<sub>2</sub> emissions up to 5.3 kg per typical winter day in Germany. 3) There is a significant correlation between the heat pump COP and the heat recovery efficiency. 4) In addition, most environmental measurements in the reference rooms in the school building fall in the comfort zone in winter, which indicates the heating energy supply based on this distributed renewable energy system could support a proper level of thermal comfort.

## **Keywords**

Ground source heat pump; Heat exchanger; Coefficient of performance (COP);  
Closed-loop borehole; CO<sub>2</sub> equivalent emission; Energy performance ratio (EPR)

Main body

## **1. Introduction**

The energy challenge, climate change and reduction of carbon emissions have substantially exerted high pressure on the building energy reductions [1-2]. In Germany, currently, buildings are responsible for approximately 40% of total annual national energy consumption and one third of national carbon emissions [3-5].

Distributed renewable energy technology used in buildings is a critical approach to effectively reduce the carbon emissions and improve energy efficiency and performance, from the both sides of energy supply and demand. Small and micro-scale distributed renewable energy systems (including building, neighbourhood or community scale), recently, have been increasingly applied in buildings due to the introduction of attractive incentives through the beneficial feed-in tariffs and government subsidies on investments [6]. Recently, Stadler enhanced the potential of renewable energy resources application in buildings, and the importance of managements of diverse energy systems, as well as the opportunities of design optimizations [6]. This study particularly discussed a small-scale distributed renewable energy system in a residential building, including several conversion and storage units. In addition, a two-step multi-objective

optimization method has been proposed in order to size both electrical and thermal energy systems, which considers thermoeconomic performance indicators to fit grid operator and consumer interests [6]. Guen et al. investigated the integration of renewable energy technologies and building renovation to improve neighbourhood-scale building energy sustainability in Hemberg, Switzerland [7]. The energy performance (thermal) in the building studied was remarkably improved through this integrated renewable system. Wind and solar energy systems could supply more than 14% of total energy demand concerning rigorous grid restrictions based on the base line, i.e., the integration of both PV panels and wind turbines along with energy storage [7]. Panchal et al. designed and developed a solar-based Rankine cycle and geothermal-based system for multi-generation of renewable energy system in residential buildings, which was applied at a community scale [8]. The energy efficiency of this multi-generation systems are higher than the single one by 20%. Using TRNSYS and an operational simulator in a building complex (Korea Institute of Energy Research (KIER),) Liu et al. [9] built the building load models used for predicting the electricity consumption with the integration of both multi-type engines and renewable energy systems including photovoltaic (PV) cells and solar collectors, fuel cells, and bio-ORC (organic Rankine cycle). This model is capable of calculating the energy consumption based on the number of running engines and their thermal efficiency, as well as the fuel consumption relevant to heating energy and the efficiency [9]. The result shows that around 5% of the produced electricity was used for the system operation, and the tool brings in reasonable

predication of electricity production, fuel consumption and working performances of systems [9]. Ikeda and Ooka proposed a new optimization strategy for the operating schedule of energy system, taking into consideration uncertainty of renewable energy sources and demand variations [10]. Implemented in an office building with a floor space of 20000m<sup>2</sup>, this study [10] illustrated that two-time steps recalculation strategy (TtsR) needed less computational time than all-time steps recalculation strategy (AtsR) to gain a quasi-optimal approach in terms of unpredicted changing conditions in the power generation and requirement. Using several case study buildings (semi-detached two-storey house, 106m<sup>2</sup> floor area) in Ireland, Moran et al. presented investigations of life cycle cost and environmental performances using the indicators for net zero energy buildings [11]. Based on the global warming potential and energy consumption, these indicators were produced for buildings with diverse heat sources including a gas boiler, biomass boiler, a domestic gas fired CHP, heat pump and renewable technologies [11]. The results showed that the future buildings should be installed with well-insulated envelopes and high-level air-tightness in order to minimize the heating load; meanwhile, the heating systems used should have deliver the minimum impact on the natural environment through adopting low carbon technologies, e.g. using heat pump or biomass boiler.

For the integrated energy systems in buildings, a proper energy performance indicator is crucial in order to effectively evaluate their energy performances and seek possible approaches to improve the performances [4-5, 12-14]. It has been regarded as a

big challenge to produce a novel energy performance indicator capable of minimizing energy consumption and without compromising comfort levels. Marta and Panao proposed a methodology for calculating the overall renewable energy fraction (OREF) used for net zero energy building, which included two performance indicators: the renewable energy ratio (RER) and the on-site energy fraction (OsEF) [12]. The results revealed that the payback credit option without considering embodied energy would theoretically generate OREF higher than 100%. OREF could be an independent indicator from direct use, fossil fuels energy carriers, other fossil fuels energy carriers [12]. Compared with the exported fraction, in addition, it will provide buildings with higher capabilities of self-consumption of on-site produced energy [12]. Bakar et al. conducted a review of the energy efficiency index (EEI) in buildings, which was used as an indicator to evaluate and measure the energy consumption [4]. In order to establish a universal index based on the standardized procedures, however, more work could be still required [4]. Guillermo et al. developed a new index of energy rating factor (ERF) in terms of building energy consumption across different seasons [13]. It has been found that buildings with distributed air conditioning (AC) units have better energy performances than those with centralized AC [13]. This could be explained by the fact that centralized units need much higher energy input, which would lead to adaptation difficulties to inconstant outdoor temperatures; at the same time, users could not effectively control those units. Another new index  $EEI_B$  proposed by Gonzalez et al. can measure the energy efficiency of both old and newly built buildings [5]. Updated in time

and using real data, this index stands for a real measure for the efficiency and therefore boosts the improvement of energy performance. Wang et al. defined a novel factor named as energy conservation ratio (ECR), targeting at the evaluation of energy performance of air conditioning unit combined with mechanical ventilation heat recovery system in Passive House buildings [14]. A higher ECR value means more energy savings. Based on CFD simulations and on-site measurements, ECR would increase with the increasing heat recovery efficiency and the reduction of temperature difference between the supply and external air.

In summary, a number of studies are currently available based on the optimization of renewable energy systems and the strategy of their operations in buildings. However, few studies focused on performance evaluations and energy indicators of the distributed renewable energy system in Passive House school buildings. In this article, a new performance assessment index to justify the renewable energy system in Passive House buildings, namely Energy Performance Ratio (EPR), has been proposed and applied. The objective of this study is to evaluate the application of this new index. The unique purpose of this study is to establish a new way to reflect energy performance of the renewable energy system based on correlations between the heat transfer level of heat pump, the energy demand, and the new index in Passive House or other similar buildings. In the following sections, the distributed renewable energy system was first introduced. Second, numerical modelling methodology and models were validated by typical on-site measured data, an energy performance ratio was proposed. Third, energy

performances of one improved distributed renewable energy system were numerically simulated, taking into account the effects of borehole outlet temperature and heat recovery efficiency. Finally, the energy performance ratio was applied and its correlations to functions of the heat pump were tested.

## **2. System description of distributed renewable energy system**

Combined with a renewable energy system including GSHP unit, a pilot project of Passive House school building has been established at a location of southern Germany (Lat.: 48°18'40", Long.: 11°53'49", Fig. 1). The GSHP system integrated in the Passive House building employs Heliotherm heat pump unit, which has a nominal capacity of 120kW for heating. The heat is transferred from the ground through a closed loop system, which is buried underground. Fig. 2 demonstrates the schematic diagram of GSHP system and Passive House building. The actual building heating load profile and sorted annual heating load for 2014 as well as the sorted annual heating load profile for 2012 and 2013 have been measured (Fig. 3). It has been found that the building demand is normally fulfilled by the GSHP system due to the sorted heating load lying within 90kW except those discrete peak loads. Meanwhile, the back-up heating energy is provided by a geothermal district heating when the local distributed renewable energy system failed to meet the heating energy demand.

## **3. Numerical modelling methodology and new EPR concept**

In order to evaluate the energy performance of renewable energy system, energy system simulation (ESS) methodology has been employed in this study. The popular



ESS program TRNSYS (transient system simulation program) [15] was applied in this article. The detailed model parameter settings are illustrated in Table 1.

### 3.1 Borehole

The closed-loop borehole (i.e. ground heat exchanger) was set up as a vertical U-tube heat exchanger, which was set up based on the practical situation. A heat carrier fluid (water in this study) is circulated via the ground heat exchanger and either rejects heat or absorbs heat from the ground depending on the temperature levels of the heat carrier fluid and the ground.

### 3.2 Heat pump

The heat pump efficiency in heating mode could be expressed as coefficient of performance (COP), which is defined by amount of thermal energy (heating capacity  $C_{heat}$ ) moved per unit of input work (power draw  $P_{heat}$ ) required as follows.

$$COP = \frac{C_{heat}}{P_{heat}} \quad (1)$$

The amount of energy absorbed from the source fluid stream  $Q_{ab}$  in heating mode is calculated by

$$Q_{ab} = C_{heat} - P_{heat} \quad (2)$$

The outlet temperatures of source ( $T_{s,o}$ ) and load ( $T_{l,o}$ ) liquid streams is then defined as

$$T_{s,o} = T_{s,i} - \frac{Q_{ab}}{m_s C_s} \quad (3)$$

$$T_{l,o} = T_{l,i} - \frac{C_{heat}}{m_l C_l} \quad (4)$$

Where  $T_{s,i}$  and  $T_{l,i}$  are the inlet temperatures of source and load liquid streams, respectively;  $m_s$  and  $C_s$  are the mass flow rate and specific heat of the liquid for the heat pump source side, separately;  $m_l$  and  $C_l$  are the mass flow rate and specific heat of the liquid for the heat pump load side, respectively.

### ***3.3 Loads imposed on the liquid stream***

The heating loads on the Passive House building have been already determined by the measurement. The building loads could be added to or subtracted from the heat carrier fluid, which will result in an outlet temperature past the interaction point in the system loop. The outlet temperature of the liquid stream could be obtained by the following:

$$T_{out} = T_{in} + \frac{Q_{load}}{mC_p} \quad (5)$$

where,  $T_{out}$  is the outlet temperature of heat carrier fluid stream leaving the building load,  $T_{in}$  represents the inlet temperature of heat carrier fluid stream arriving the building load,  $Q_{load}$  means the rate where energy is appended to or removed from the heat carrier fluid stream,  $m$  is the rate at which heat carrier fluid flows past the load, and  $C_p$  is the specific heat of the heat carrier fluid.

### ***3.4 Water-water heat exchanger***

In order to improve the energy efficiency of renewable energy system, a water-water heat exchanger has been proposed to append in between the source side and load side of the heat pump, illustrated in Fig. 4. Based on energy balance of the heat

recovery facility transferring the borehole outlet water and heat pump load return water could be represented in the following relation,

$$M_{\text{bout}}\rho_{\text{bout}}C_{\text{bout}}(T_{\text{sin}} - T_{\text{bout}}) = M_{\text{lre}}\rho_{\text{lre}}C_{\text{lre}}(T_{\text{lin}} - T_{\text{lre}}) \quad (6)$$

where,  $M_{\text{bout}}$  and  $M_{\text{lre}}$  represent the borehole outlet entering and heat pump load side return water flow volume rates ( $\text{m}^3/\text{h}$ ) by the system, respectively. Their specific thermos-physics properties have been respectively determined by  $\rho_{\text{bout}}$  and  $\rho_{\text{lre}}$  ( $\text{kg}/\text{m}^3$ ),  $C_{\text{bout}}$  and  $C_{\text{lre}}$  ( $\text{kJ}/\text{kgK}$ ).  $T_{\text{sin}}$ ,  $T_{\text{bout}}$ ,  $T_{\text{lin}}$  and  $T_{\text{lre}}$  mean the water temperature entering the source side of heat pump, the borehole outlet temperature, the water temperature entering the load side of heat pump and the water temperature returning from the load, respectively. In addition, the volumes of water flow rates across the heat exchanger should be maintained balanced in this study, i.e.,

$$M_{\text{bout}} = M_{\text{lre}} \quad (7)$$

Assuming that specific heat capacity and density for the water in the range of the investigated temperatures in this paper, energy balance equation could be further written as,

$$T_{\text{sin}} - T_{\text{bout}} = T_{\text{lin}} - T_{\text{lre}} \quad (8)$$

The actual heat transfer depends on the specified effectiveness  $\eta$ , which is defined as based on Equ. (8),

$$\eta = \frac{T_{\text{lin}} - T_{\text{lre}}}{T_{\text{lre}} - T_{\text{bout}}} \times 100\% = \frac{T_{\text{sin}} - T_{\text{bout}}}{T_{\text{lre}} - T_{\text{bout}}} \times 100\% \quad (9)$$

### 3.5 New EPR concept

A new energy performance index of renewable energy system has been proposed in this study, which combines COP of heat pump with water-water heat recovery efficiency  $\eta$  and is then defined by  $\text{COP} * \eta$  – energy performance ratio (EPR). It determines the whole energy efficiency of present renewable energy system including both of the GSHP and heat recovery unit. In the Section 5, EPR will be investigated and could be as an important factor to evaluate the energy performance of proposed renewable energy system.

#### **4. Validation of ESS models**

It is still necessary to validate the ESS program before it was extensively adopted as the tool of investigation, even though the present numerical methodology was successfully applied in varieties of studies [16-20]. The validation was completed by comparing the ESS results with experimental data obtained by the actual measurements from a sensor monitoring database Medview 2. Two steps have been carried out. Firstly, the simulation model has been also validated via comparing the COP values of model prediction with actual test. The GSHP operation schedule is completely identical to the actual situation, i.e., it runs from 7 am to 9 pm during the workdays. The heat meter applied is Grundfos Magna 3 VFS with an accuracy of  $\pm 2.5\%$  of the measured values. There are two temperature sensors Pt500 with an accuracy of  $\pm 0.5\%$  of the measured values, which are installed in outlet of borehole. The electrical power meter is Aidon series 6000 with an accuracy of  $\pm 1.5\%$  of the measured values. Fig. 5(a) presents the COP comparison of simulation results and actual measurement data on Jan. 15<sup>th</sup>, 2015.

Seen from Fig. 5(a), the predicted simulation results demonstrate a very good agreement with the actual test data. The maximum discrepancy is approximately  $\pm 6\%$ , which could demonstrate the reliability and accuracy of the following numerical simulation investigations. Secondly, the borehole outlet temperature levels have been compared between ESS predicted results and actual measurement data, as illustrated in Fig. 5(b). It shows the agreement between simulation results and measurement data has been reasonably achieved, which will ensure the reliability of the following numerical simulations.

## **5. Results and discussion**

Energy performance of renewable energy system is substantially affected by the borehole outlet temperature and heat recovery efficiency. Therefore, it is necessary to evaluate the effects of borehole outlet temperature and heat recovery efficiency. In addition, the new energy performance index of renewable energy system, i.e.,  $COP*\eta$  and its detailed correlation with heat pump heat transfer to the load will be also investigated in this study.

### **5.1 Effect of borehole outlet temperature on energy system**

Borehole outlet temperature level will determine source side entering temperature of heat pump and significantly affects the COP of heat pump and the heating capacity. Thus, it is very important to investigate the effect of borehole outlet temperature [21].

Fig. 6(a) demonstrates borehole and heat pump source side outlet temperatures as

functions of time on Jan. 15<sup>th</sup>, 2015. As shown in Fig. 6(a), the heat pump source outlet temperature is proportional to the borehole outlet temperature, whilst the temperature difference in between is around 3 °C. It means the evaporator of heat pump absorbs heat from water (equivalent to around 3 °C) from the source side. Fig. 6(b) illustrates heat pump heating capacity, electrical power and COP as functions of borehole outlet temperature. It could be seen that COP values lie within the ranges from around 3.4 to 4.4. In addition, COP is positively proportional to the heating capacity of heat pump; however, it is negatively proportional to the electrical power of heat pump, which is corresponding to actual heat pump COP definition and could be demonstrated by using the exergy efficiency of the heat pump compressor  $\eta_{comp}$ , i.e.,  $\eta_{comp}$  is negatively/positively proportional to the electrical power/flow exergy rate changing of heat pump.

## 5.2 Effect of heat recovery efficiency on energy system

The return heat carrier water from the load side of heat pump is first delivered through the water-water heat exchanger to pre-heat the entrained borehole water, and the recovery efficiency of the heat exchanger could take the effect on the operation of the heat pump. The entire renewable energy performance could be also highly affected by the heat recovery efficiency. It is therefore significant to investigate the effects of the heat recovery efficiency on COP of heat pump, heating energy output and electrical power of heat pump, costs of electricity, and CO<sub>2</sub> equivalent emissions.

Fig. 7 illustrates the comparison of various COP values as functions of the heat

recovery efficiency. As regards Fig. 7, COP of heat pump increases with the enhancement of heat recovery efficiency. Compared with the case without heat exchanger, average COP could be enhanced around 3.1%  $((3.97 - 3.85)/3.85)$  for the case with the heat recovery of 80% in a typical winter day.

Fig. 8(a) demonstrates the comparison of different heat pump heating output and electrical power as functions of heat recovery efficiency. Observed from Fig. 8(a), almost a linearly increasing function or a decaying function between the heat recovery rate and heat pump heating output or electrical power, respectively, could be set up. As the heat recovery efficiency equals 0.9, heat pump heating output and electrical power could increase by around 4.2%  $((81.26 \text{ kW} - 78 \text{ kW})/78 \text{ kW})$  and shrink by approximately 1.0%  $((20.42 \text{ kW} - 20.26 \text{ kW})/20.26 \text{ kW})$ , respectively, compared with that of no heat exchanger. Fig. 8(b) shows the normalized heat pump electrical power consumption for the case without heat recovery as functions of heat recovery efficiency. Almost linearly decaying function between heat recovery efficiency and normalized heat pump electrical power consumption could be observed. Compared with the case without heat recovery unit, normalized heat pump electrical power consumption could be reduced around 3.6%  $((20.26 \text{ kW} - 19.6 \text{ kW})/19.6 \text{ kW})$  for the case of 0.9 as the heat recovery rate.

Fig. 9 indicates the heat pump electricity energy consumption (kWh; broken red curve), CO<sub>2</sub> equivalent emission (kg; broken black curve) and electricity costs (Euro; broken blue curve), which are the functions of heat recovery efficiency based on the

results of Fig. 8(b). The three values are displayed as ordinates. The latest CO<sub>2</sub> equivalent emission factor is 0.527 kg/kWh in Germany [22]. The average mixed electricity price is 0.285 €/kWh in Germany [23]. As for Fig. 9, almost linear decaying functions between electricity energy consumption, CO<sub>2</sub> equivalent emission, electricity costs and heat recovery efficiency could be built. Heat pump electrical power consumption could be reduced by around 3.4%  $((304 \text{ kWh} - 294 \text{ kWh})/294 \text{ kWh})$  or 10 kWh for the case of 0.9 as the heat recovery rate in comparison with the case of without heat exchanger per one typical winter day. Compared with the case of no heat recovery, CO<sub>2</sub> equivalent emission and electricity costs could be decreased approximately 5.3 kg  $(160.2 \text{ kg} - 154.9 \text{ kg})$  and 2.9 €  $(86.6 \text{ €} - 83.7 \text{ €})$ , respectively, for the case of 0.9 as the heat recovery efficiency. The heating period in local area is from October 1<sup>st</sup> to April 30<sup>th</sup>, i.e., approximately 176 days except public and school holidays [3, 24]. Therefore, compared with the case without heat recovery, heat pump electrical power consumption could be reduced by around 1760 kWh per year, while CO<sub>2</sub> equivalent emission and electricity costs could be dropped about 932.8 kg  $(5.3 \text{ kg} * 176)$  and 510.4 €  $(2.9 \text{ €} * 176)$ , respectively, for the case of the heat recovery efficiency with 0.9.

### **5.3 Effect of renewable energy system on thermal comfort**

Indoor environment and human thermal comfort play a vital role in learning and teaching in school buildings, since they could assist students to engage in leaning activities which enhance their learning performance, including the concepts understanding, attitudes of learning and problem analysing and solving abilities etc. [25].



It is thus necessary to study the influence of proposed renewable energy system performance on thermal comfort and evaluate whether the indoor environment could fulfil thermal comfort requirement in this Passive House school building.

Fig. 10(a) and (b) demonstrate the indoor temperature and relative humidity in the reference room 3.3 and 2.28, as well as their corresponding positions in the comfort zone in winter 2015/2016. Observed from both figures, all measured data completely lie within comfortable zone, which illustrates that the indoor environment could provide with higher levels of thermal comfort in winter. In addition, it also denotes that the proposed renewable energy system could meet the heating demand in this Passive House school building in winter.

#### **5.4 Effect of combination with heat recovery efficiency and COP**

Heat exchanger facility could simultaneously enhance the entering temperature level of source side of heat pump and the COP of heat pump. In this study, the COP as functions of efficiency of the water-water heat exchanger facility is investigated and demonstrated in Fig. 11(a), considering its value from 0 to 1. As shown in Fig. 11(a), COP values linearly increase with the enhancement of the heat recovery efficiency. Comparing with the case without heat recovery facility, COP could improve around 3.9%  $((4.0 - 3.85)/3.85)$  for the case of heat recovery efficiency of 100%. Meanwhile, a linear function  $COP = 0.15 * \eta + 3.85$  could be set up.

Water transferred through the borehole will be firstly delivered passing the heat recovery unit to pre-heat the entrained water source, and the heat recovery efficiency of

the heat recovery facility could take the effect on the operation of the heat pump unit. Various situations of COP and heat recovery efficiency, i.e., energy performance ratio for renewable energy system:  $COP*\eta$ , have been correlated in terms of the heat pump heat transfer to the load, shown in Fig. 11(b),

$$\ln(COP*\eta) = 0.64 \times P_{load} - 50.71 \quad (10)$$

As expected, a linear function between the natural logarithm of energy performance ratio -  $COP*\eta$  and the heat pump heat transfer to the load could be set up. This has demonstrated that better energy performance of the renewable energy system could be reflected by the higher heat pump heat transfer level to the load (Passive House building) with the enhancement of energy performance ratio. On the other hand, energy consumption of the distributed renewable energy system could be reduced when the energy performance ratio increases. In addition, the integrated renewable energy system could become more efficient when the heat recovery efficiency gradually approaches 1.0.

## 6. Conclusions and future work

In heating season, the closed-loop borehole, heat pump unit and water-water heat exchanger facility are jointly in operation, which aim to reduce the energy consumption and improve the energy performance. The performances of distributed renewable energy system and indoor thermal comfort in the Passive House school building have been experimentally and numerically investigated in this study. Also, ESS methodology and numerical models have been validated by typical on-site measured data, even though

some observed discrepancies appeared between ESS results and measurements. Several important findings are as follows:

(1) Increasing the heat recovery efficiency of water-water heat exchanger facility could not only enhance linearly COP of heat pump, but also save 10 kWh electricity energy and around 3 € electricity costs, respectively, and reduce CO<sub>2</sub> emissions 5.3 kg per typical winter day in Germany, by a comparison between the case of heat recovery efficiency with 0.9 and the case having no heat recovery. Annually, it will then save 1760 kWh electrical energy, and decrease 932.8 kg CO<sub>2</sub> equivalent emissions and 510.4 € electricity costs.

(2) The proposed distributed renewable energy system could provide adequate heating energy for ensuring proper thermal comfort in this Passive House school building. Most measured data in the reference rooms in this Passive House school building fall within the comfort zone in winter.

(3) COP of the heat pump unit and the heat recovery efficiency have been correlated in terms of the heat pump heat transfer to the load. It has been found that better energy performance of the distributed renewable energy system could be reflected by the higher heat transfer level of heat pump to the load (Passive House building) with the enhancement of energy performance ratio.

This research could benefit for the design and optimization of distributed renewable energy system integrated with Passive House building. Further investigations, including development of thermal storage and demand response strategy for the Passive House

building combined with renewable energy system, are currently under the way.

## **Acknowledgements**

This research was financially supported by the German Federal Environmental Foundation (Deutsche Bundesstiftung Umwelt, DBU AZ 26170/02-25 & 35), China Agricultural University Excellent Talents Plan, and Fundamental Research Funds for the Central Universities in China (Grant No. 2018QC174). The authors also appreciate constructive and valuable comments provided by reviewers.

## **References**

- [1] CCC, 2016. Next step for UK heat policy, London: Committee on Climate Change.
- [2] Y. Wang, J. Kuckelkorn, F. Y. Zhao, H. Spliethoff, W. Lang. A state of art of review on interactions between energy performance and indoor environment quality in Passive House buildings. *Renewable and Sustainable Energy Reviews* 72 (2017) 1303-1319.
- [3] Y. Wang. Optimization for building control systems of a school building in passive house standard. PhD Dissertation, Media Technical University of Munich, Munich, 2015.
- [4] N. Bakar, M. Hassan, H. Abdullah, et al. Energy efficiency index as an indicator for measuring building energy performance: A review. *Renewable and Sustainable Energy Reviews* 44 (2015) 1-11.
- [5] A. Gonzalez, J. Diaz, A. Caamano, M. Wilby. Towards a universal energy efficiency

index for buildings. *Energy and Buildings* 43-4 (2011) 980-987.

[6] P. Stadler, A. Ashouri, F. Marechal. Model-based optimization of distributed and renewable energy systems in buildings. *Energy and Buildings* 120 (2016) 103-113.

[7] M. L. Guen, L. Mosca, A. T. D. Perera, etc. Improving the energy sustainability of a Swiss village through building renovation and renewable energy integration. *Energy and Buildings* 158 (2018) 906-923.

[8] S. Panchal, I. Dincer, M. Agelin-Chaab. Analysis and evaluation of a new renewable energy based integrated system for residential applications. *Energy and Buildings* 128 (2016) 900-910.

[9] J. Liu, D. Chung, M. Chung, Y. Im. Development of load models and operation simulator for a building complex with mixtures of multi-type engines and renewable devices. *Energy and Buildings* 158 (2018) 831-847.

[10] S. Ikeda, R. Ooka. A new optimization strategy for the operating schedule of energy systems under uncertainty of renewable energy sources and demand changes. *Energy and Buildings* 125 (2016) 75-85.

[11] P. Moran, J. Goggins, M. Hajdukiewicz. Super-insulate or use renewable technology? Life cycle cost, energy and global warming potential analysis of nearly zero energy buildings (NZEB) in a temperate oceanic climate. *Energy and Buildings* 139 (2017) 590-607.

[12] J. N. Marta, O. Panao. The overall renewable energy fraction: An alternative performance indicator for evaluating Net Zero Energy Buildings. *Energy and Buildings*

127 (2016) 736-747.

[13] E. Guillermo, A. Carlos, P. Elisa. New indices to access building energy efficiency at the use stage. *Energy and Buildings* 43 (2011) 476-484.

[14] Y. Wang, J. M. Kuckelkorn, F. Y. Zhao, M. L. Mu, D. L. Li. Evaluation on energy performance in a low-energy building using new energy conservation index based on monitoring measurement system with sensor network. *Energy and Buildings* 123 (2016) 79-91.

[15] TRNSYS. A Transient Simulation Program, Version 17, University of Wisconsin Solar Energy Laboratory, Madison, WI, 2012.

[16] Y. Wang, J. Kuckelkorn, F. Y. Zhao, etc. Evaluation on classroom thermal comfort and energy performance of passive school building by optimizing HVAC control systems. *Building and Environment* 89 (2015) 86-106.

[17] L. T. Terziotti, M. L. Sweet, J. T. Mcleskey Jr. Modelling seasonal solar thermal energy storage in a large urban residential building using TRNSYS 16. *Energy and Buildings* 45 (2012) 29-31.

[18] E. Ampatzi, I. Knight. Modelling the effect of realistic domestic energy demand profiles and internal gains on the predicted performance of solar thermal systems. *Energy and Buildings* 55 (2012) 285-298.

[19] S. Firlag, S. Murray. Impact of airflows, internal heat and moisture gains on accuracy of modelling energy consumption and indoor parameters in passive building. *Energy and Buildings* 64 (2013) 372-383.

- [20] B. L. Gowreesunker, S. A. Tassou, M. Kolokotroni. Coupled TRNSYS-CFD simulations evaluating the performance of PCM plate heat exchangers in an airport terminal building displacement conditioning system. *Building and Environment* 65 (2013) 132-145.
- [21] F. J. Ju, X. W. Fan, Y. P. Chen, et al. Experiment and simulation study on performances of heat pump water heater using blend of R744/R290. *Energy and Buildings* 169 (2018) 148-156.
- [22]<https://www.umweltbundesamt.de/daten/energie/energiebedingte-emissionen#textpart-3>
- [23] <https://www.kwh-preis.de/strom/strompreise>
- [24] J. M. Kuckelkorn, A. Kirschbaum, F. Volz, M. Biank. Neubau der Fach- und Berufsoberschule in Erding: Nachhaltiges Passivhaus mit extrem niedrigem Gesamt-Primaerenergiebedarf: Dokumentation der Monitoringphase. Abschlussbericht, Erding, 2015.
- [25] M. Puteh, M. H. Ibrahim, M. Adnan, etc. Thermal comfort in classroom: constraints and issues. *Procedia – Social and Behavioral Sciences* 46 (2012) 1834-1838.

Figure 1



Fig. 1: Façade picture of Passive House building in southern Germany in winter.



Figure 2

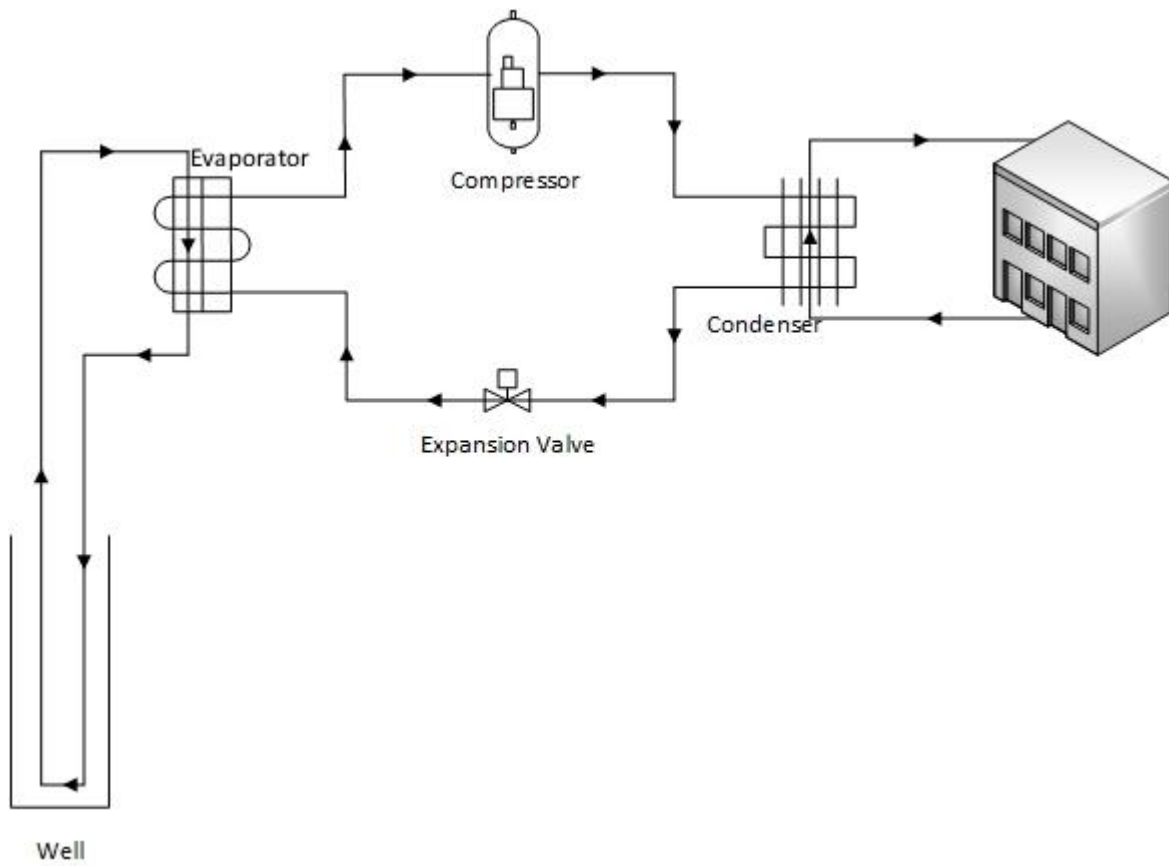


Fig. 2: Schematic diagram of GSHP (including closed-loop borehole and heat pump unit) system and Passive House building.

Figure 3

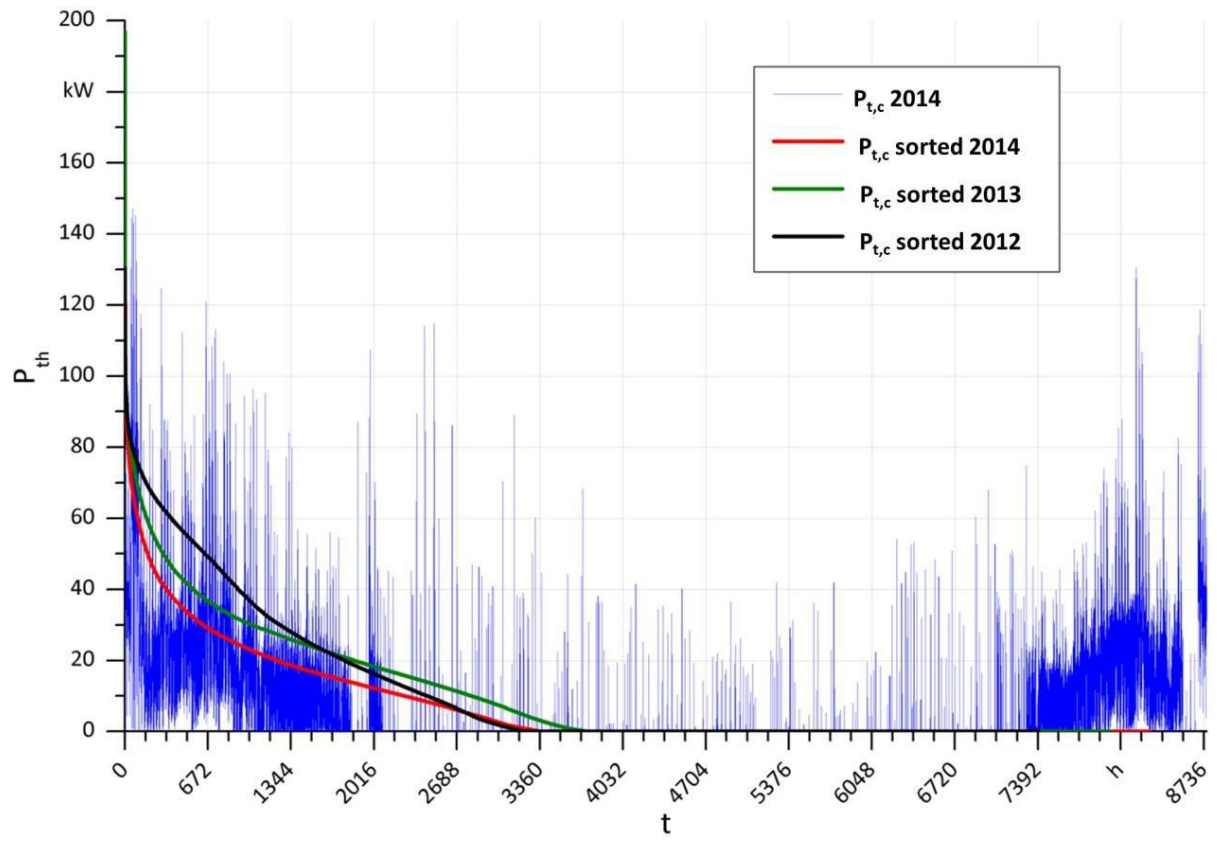


Fig. 3: Heating load  $P_{th}$  profile of 2014 and its sorted load  $P_{t,c}$  as well as sorted loads from 2013 and 2012.

Figure 4

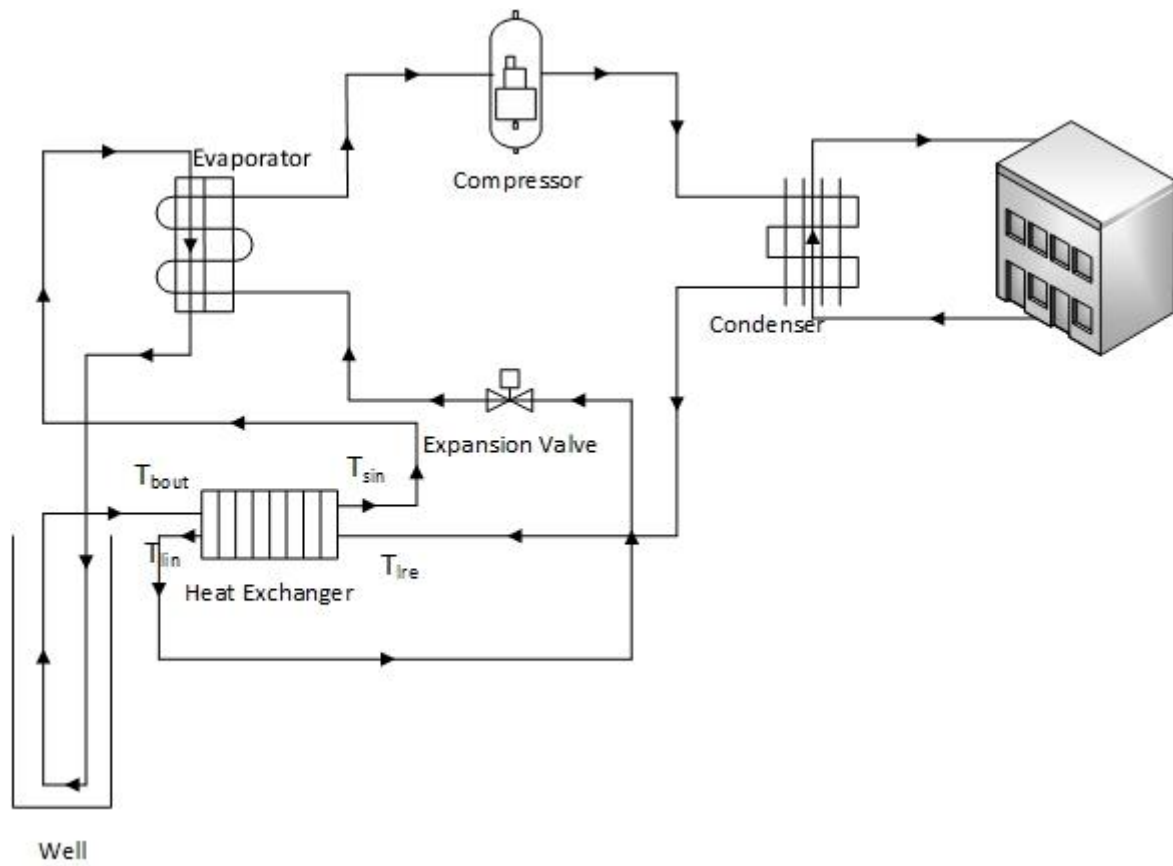
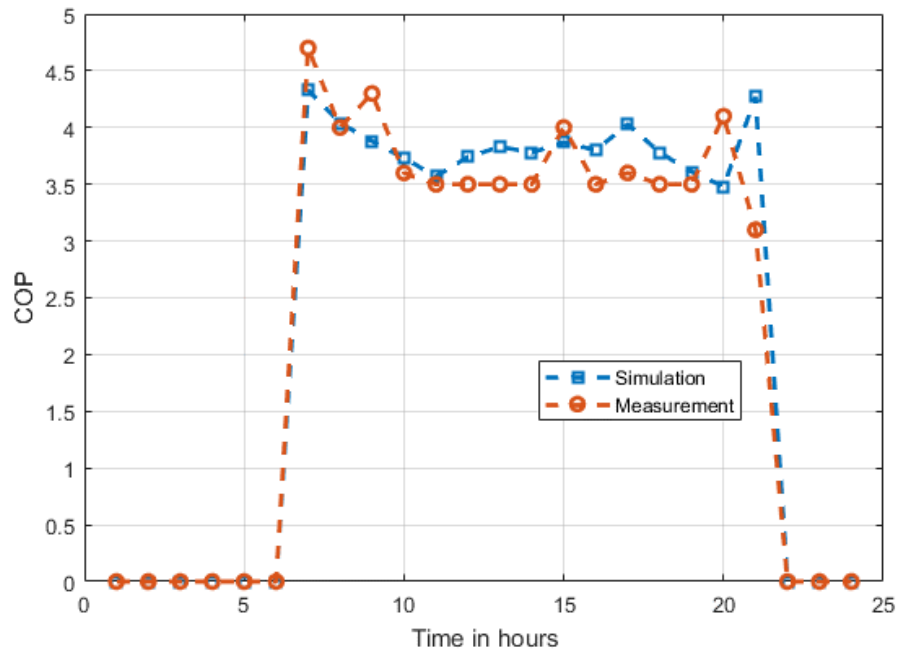


Fig. 4: Schematic diagram of GSHP (including closed-loop borehole and heat pump) system, water-water heat exchanger and Passive House building.

Figure 5



(a)

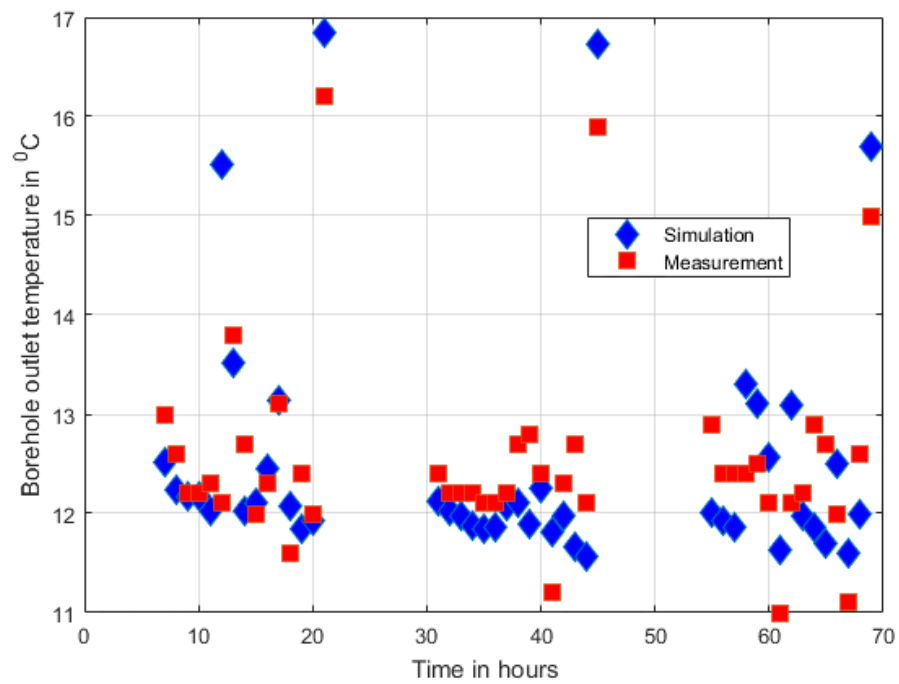
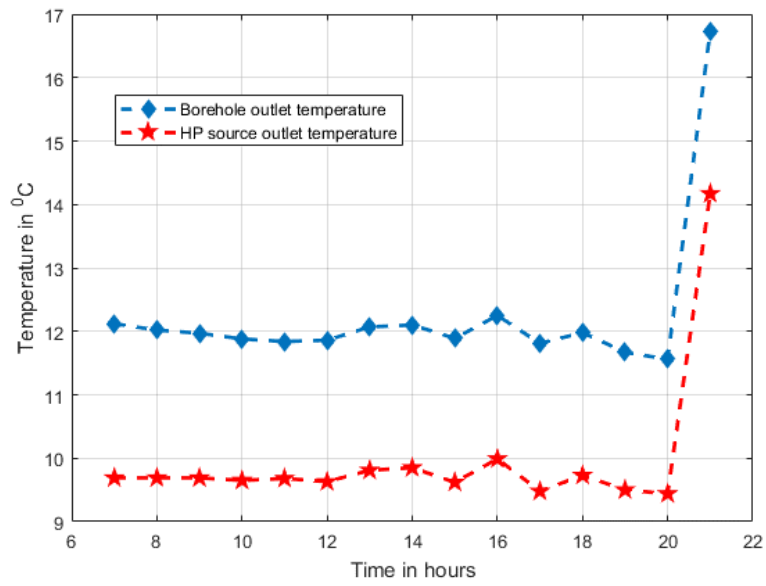
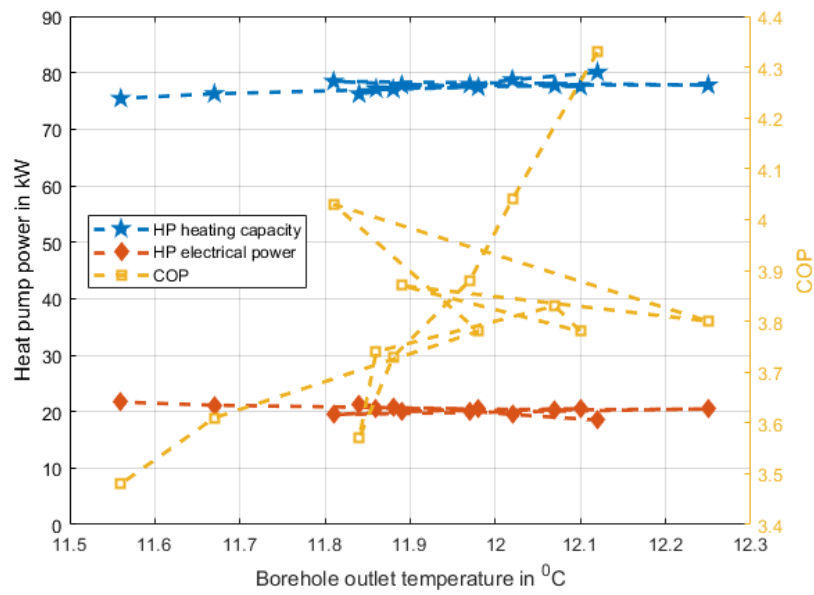


Fig. 5: COP comparison (a) of simulation results and actual measurement data on Jan. 15<sup>th</sup>, 2015, and borehole outlet temperature comparison (b) of simulation results and actual measurement data on Jan. 14<sup>th</sup> to 16<sup>th</sup>, 2015.

Figure 6



(a)



(b)

Fig. 6: Borehole and heat pump source side outlet temperatures as functions of time (a) and heat pump heating capacity, electrical power and COP as functions of borehole outlet temperature (b).

Figure 7

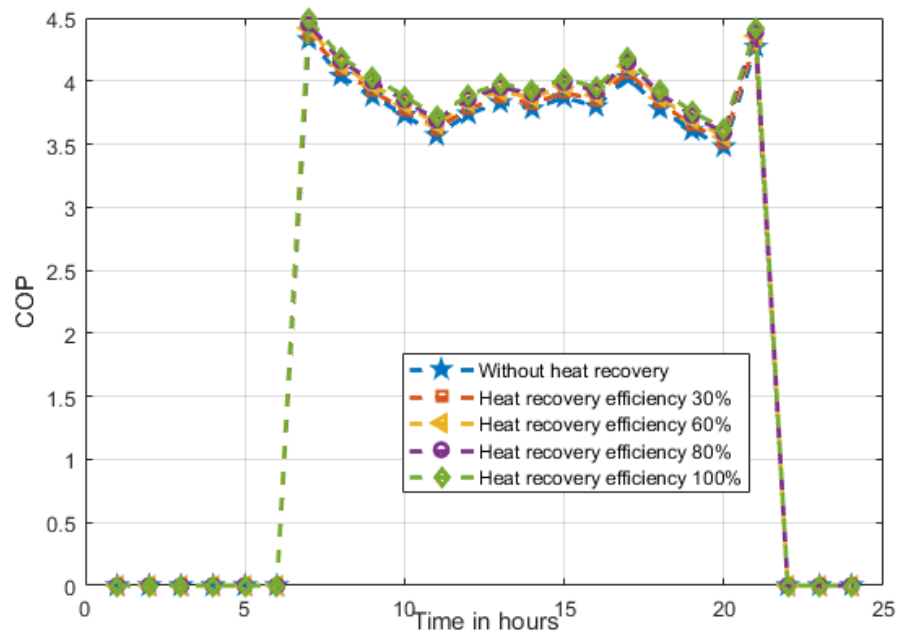
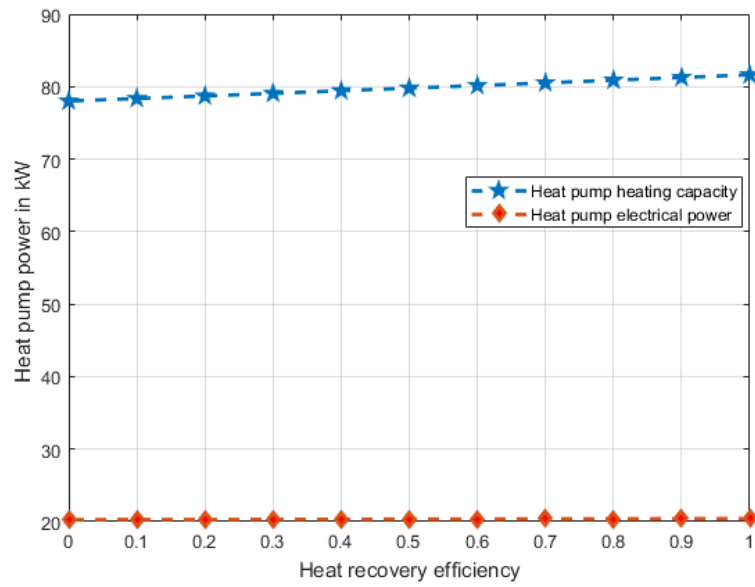
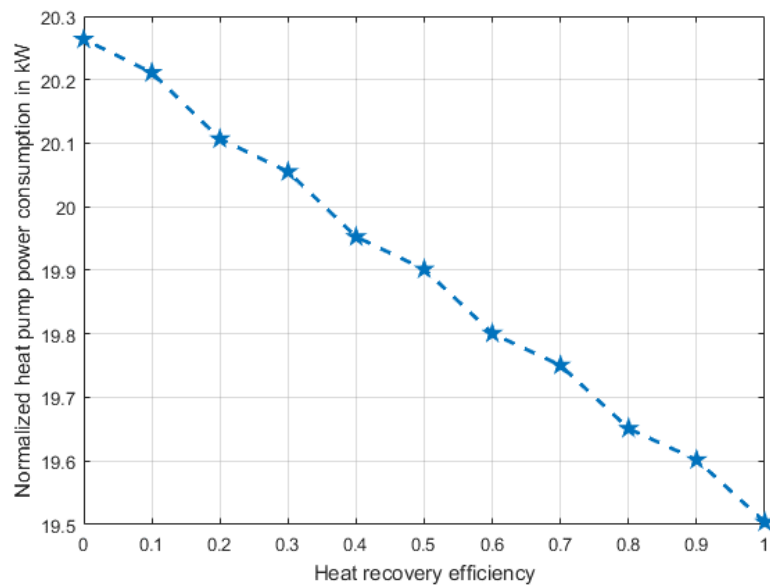


Fig. 7: Comparison of different COP values as functions of heat recovery efficiency

Figure 8



(a)



(b)

Fig. 8: Comparison of different heat pump heating capacity and electrical power values (a) and normalized heat pump electrical power consumption values for the case of without heat exchanger as functions of heat recovery efficiency.

Figure 9

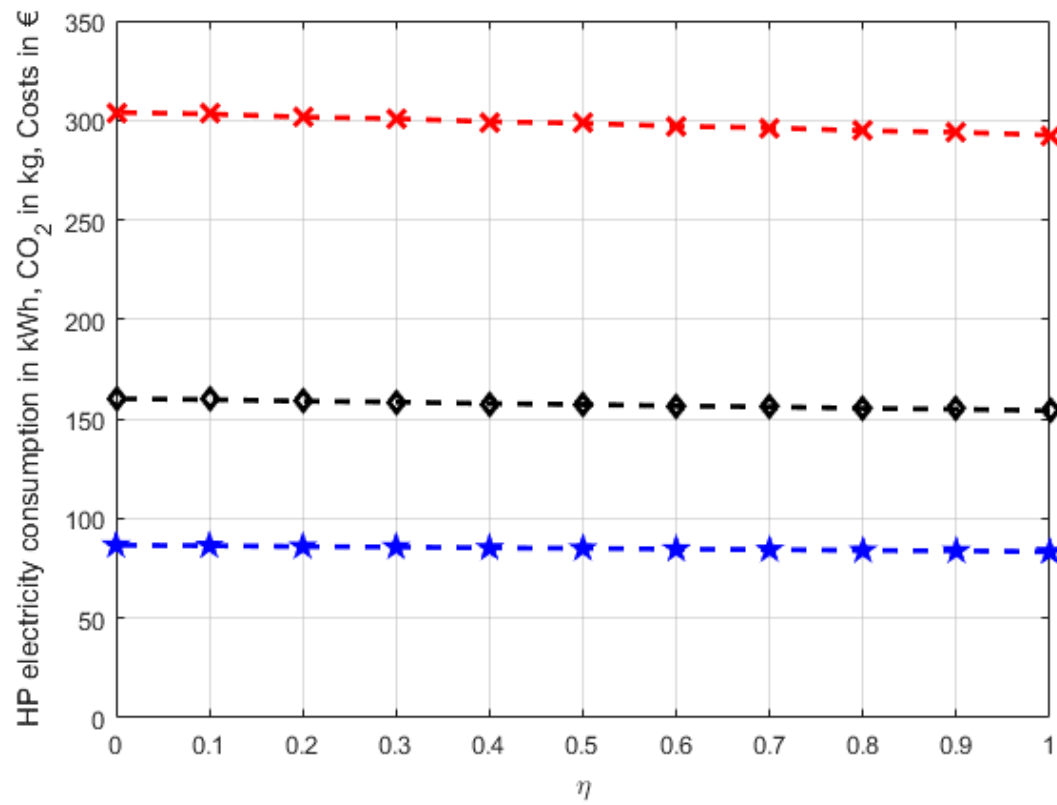
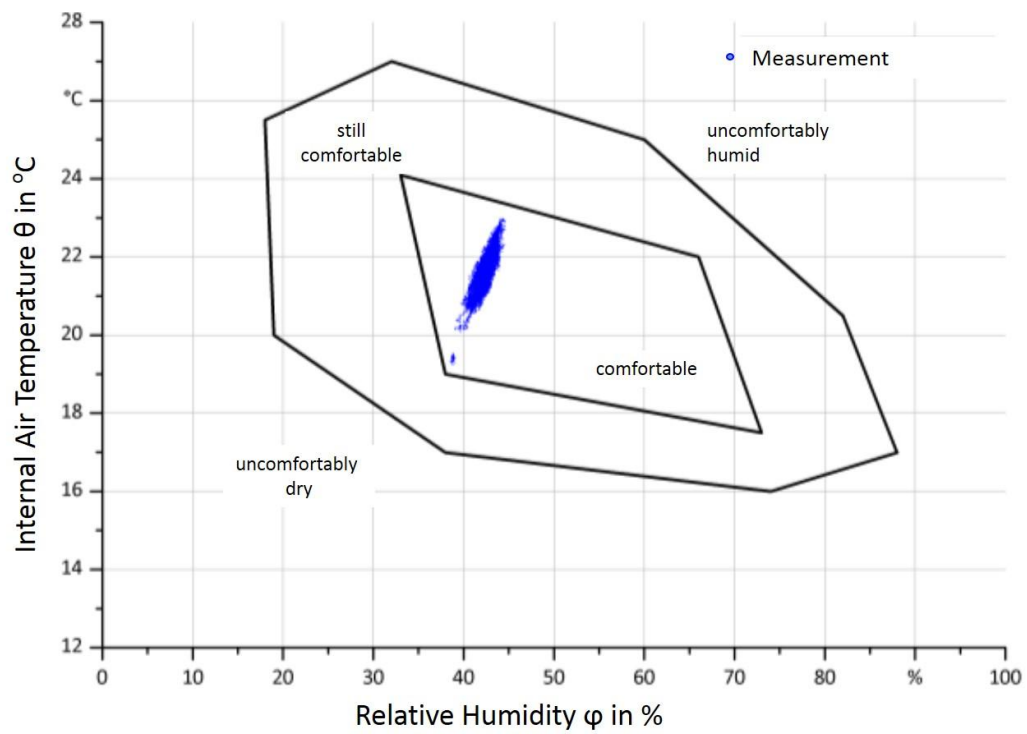


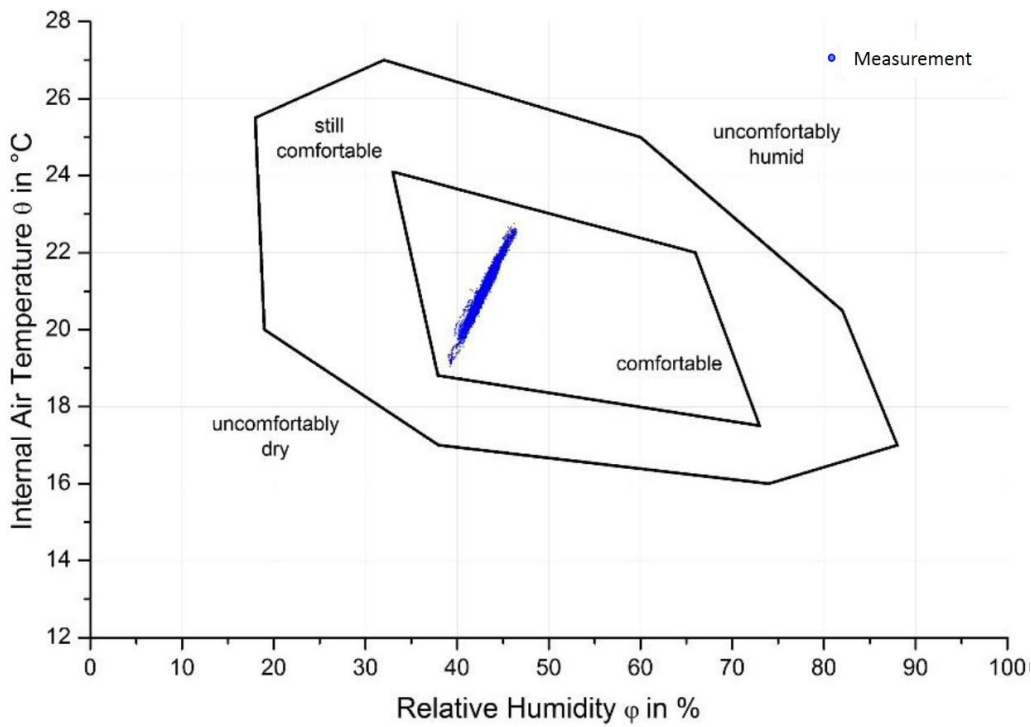
Fig. 9: Heat pump electricity energy consumption (broken red curve) in kWh, CO<sub>2</sub> equivalent emission (broken black curve) in kg and electricity costs (broken blue curve) in Euro as functions of heat recovery efficiency based on Fig. 8(b).



Figure 10



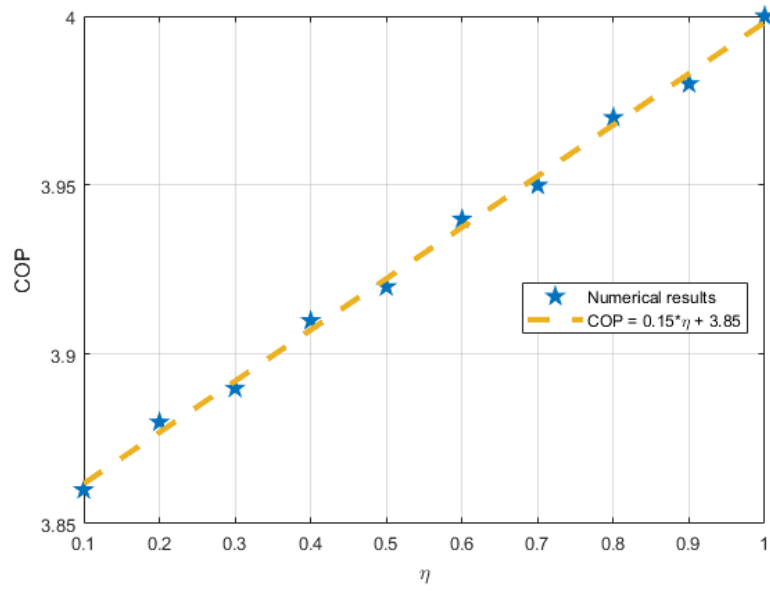
(a)



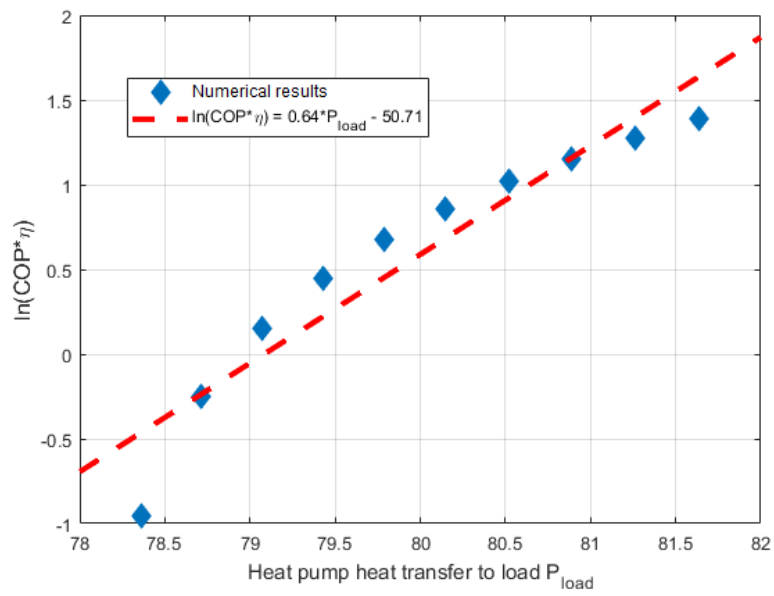
(b)

Fig. 10: Reference room 3.3 (a) and reference room 2.28 (b) indoor temperature and relative humidity as well as the corresponding comfort zone in winter 2015/2016.

Figure 11



(a)



(b)

Fig. 11: COP as functions of heat recovery efficiency (a) and correlations of COP and heat recovery efficiency  $\eta$  as functions of heat pump heat transfer to load (b).

Table 1

**Table 1:** Main components and parameter settings (default condition).

Name	Main parameters
Borehole	Depth: 30 m; Radius: 0.4; Storage heat capacity: 2000 kJ/m <sup>3</sup> K; Reference borehole flow rate: 7 kg/s; Insulation thermal conductivity: 0.3 W/mK
Heat pump	Load specific heat: 4.19 kJ/kgK; Rated heating capacity: 120 kW; Rated electricity power: 25 kW
Loads	Fluid specific heat: 4.19 kJ/kgK; Inlet flow rate: 8.5 kg/s
Heat exchanger	Specific heat of fluid: 4.19 kJ/kgK; Hot side flow rate: 100 kg/h; Cold side flow rate: 100 kg/h